A Case Study of Non-Newtonian Viscosity of Blood Through Atherosclerotic Artery

Sapna Ratan Shah
Department of Mathematics, Harcourt Butler Technological Institute,
208002 Kanpur, India

Abstract: Presented herein the study of rheological character of blood flow and investigate the significance of non-Newtonian viscosity of blood through stenosed artery by assuming blood as Bingham Plastic and Casson's Fluid Models. By using Matlab software equations have been solved and the graphs have plotted. And the graphs show that blood pressure increases very significantly in the upstream zone of the stenotic artery as the degree of the stenosis area severity increases. It is also shown that the non-Newtonian behaviour of blood has significant effects on the velocity profile of the blood flow and the magnitude of the wall shear stresses. It has been concluded in this study that the Casson's fluid model is more realistic in comparison to Bingham Plastic Fluid Model.

Key words: Non-Newtonian, apparent viscosity, resistance to flow, Bingham Plastic Fluid model, Casson's Fluid Model, India

INTRODUCTION

For many decades, cardiovascular disease has been one of the most severe diseases causing a large number of deaths worldwide each year especially in developed countries. Most of the cases are associated with some form of abnormal flow of blood in stenotic arteries. In the presence of stenosis or atherosclerosis (Fig. 1), the normal blood flow through the artery is disturbed resulting in blood recirculation and wall shear stress oscillation near the stenosis.

The heart has to increase the blood pressure to impel the blood passing through the narrowing region so as to enforce the blood circulation. If the heart works too hard and the blood cannot flow well, heart attack may occur. In order to understand the blood flow behaviour in arteries so as to provide sufficient information for clinical purposes intensive research has been carried out worldwide for both normal and stenotic arteries. In the series of the studies (Texon, 1957; May *et al.*, 1963; Hershey and Cho, 1966; Young, 1968; Forrester and Young, 1970; Caro *et al.*, 1971; Fry, 1972; Young and Tsai, 1973; Lee, 1974; Kirkeeide *et al.*, 1977), the effects on the cardiovascular system can be understood by studying the blood flow in its vicinity. In these studies the behavior of the blood has been considered as a Newtonian fluid. However, it may be noted that the blood does not behave as a Newtonian fluid under certain conditions. It is generally accepted that the blood being a suspension of cells, behaves as a non-Newtonian fluid at low shear rate

Fig. 1: Arterial atherosclerosis

(Charm, 1965; Hershey and Cho, 1966; Whitmore, 1968; Cokelet, 1972; Lih, 1975; Shukla *et al.*, 1980). It has been pointed out that the flow behaviour of blood in a tube of small diameter (<0.2 mm) and at <20 sec^{-1} shear rate can be represented by a power-low fluid (Hershey and Cho, 1966; Charm, 1965). It has also been suggested that at low shear rate (0.1 sec^{-1}) the blood exhibits yield stress and behaves like a Casson Model fluid (Casson, 1959; Reiner and Baldair, 1959). For blood flows in large arterial vessels (vessel diameter = 1 mm) LaBarbera (1990) and Jung *et al.* (2004) which can be considered as a large deformation flow, the predominant feature of the rheological behavior of blood is its shear rate dependent viscosity and its fact on the hemodynamics of large arterial vessel flows has not been understood well.

In this study the effect of non-Newtonian viscosity of blood through stenosed artery has been investigated. The effect of stenosis on the resistance to flow, apparent

viscosity and wall shear stress in an artery by considering the blood as a Bingham Plastic fluid and Casson's Model fluids have also been determined and to examine the effect of stenosis shape parameter, researchers considered blood flow through an axially non-symmetrical but radially symmetric stenosis such that the axial shape of the stenosis can be change just by varying a parameter, stenosis shape parameter (m).

FORMULATION OF THE PROBLEM

In the present analysis, it is assumed that the stenosis develops in the arterial wall in an axially non-symmetric but radially symmetric manner and depends upon the axial distance z and the height of its growth. In such a case the radius of artery, R (z) can be written as follows (Fig. 2):

$$\left. \begin{array}{l} \dfrac{R(z)}{R_0} = 1 - A[L_0^{(m-1)}(z-d) - (z-d)^m], \quad d \le z \le d + L_0 \\ = 1, \qquad\qquad\qquad\qquad\qquad\qquad\qquad \text{otherwise} \end{array} \right\} \tag{1}$$

Where:

R (z) and R_0 = The radius of the artery with and without stenosis, respectively
L_0 = The stenosis length
d = Indicates its location
$m \ge 2$ = A parameter determining the stenosis shape and is referred to as stenosis shape parameter

Axially symmetric stenosis occurs when m = 2 and a parameter A is given by:

$$A = \frac{\delta}{R_0 L_0^m} \frac{m^{m/(m-1)}}{(m-1)}$$

where, δ denotes the maximum height of stenosis at z = $d+L_0/m^{1/(m-1)}$. The ratio of the stenosis height to the radius of the normal artery is much less than unity.
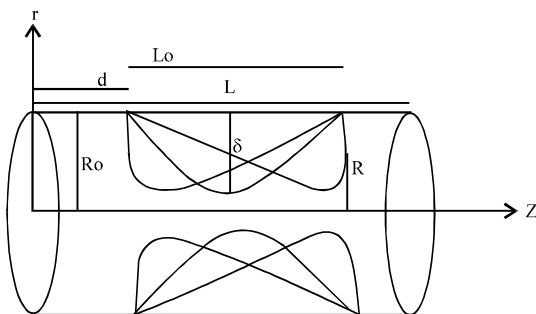

Fig. 2: Geometry of stenosis

CONSERVATION EQUATION AND BOUNDARY CONDITION

The equation of motion for laminar and incompressible, steady, fully-developed, one-dimensional flow of blood whose viscosity varies along the radial direction in an artery reduces to:

$$\left. \begin{array}{l} 0 = -\dfrac{\partial P}{\partial r} + \dfrac{1}{r}\dfrac{\partial (r\tau)}{\partial z}, \\ \\ 0 = -\dfrac{\partial P}{\partial r}, \end{array} \right\} \tag{2}$$

Where:
(z, r) = Co-ordinates with z measured along the axis
r = Normal to the axis of the artery

Following boundary conditions are introduced to solve the above equations:

$$\left. \begin{array}{ll} \partial u/\partial r = 0 & \text{at } r = 0 \\ u = 0 & \text{at } r = R(z) \\ \tau \text{ is finite} & \text{at } r = 0 \\ P = P_0 & \text{at } z = 0 \\ P = P_L & \text{at } z = L \end{array} \right\} \tag{3}$$

BINGHAM PLASTIC FLUID MODEL

For Bingham plastic fluid, the stress-strain relation is given by:

$$\tau = \tau_0 + \mu\left(-\frac{du}{dr}\right) \tag{4}$$

$$\text{where} \quad \tau = \left(-\frac{dp}{dz}\frac{r}{2}\right), \ \tau_0 = \left(-\frac{dp}{dz}\frac{R_P}{2}\right)$$

Where:
u = The axial viscosity
μ = The viscosity of fluid
(-dp/dz) = The pressure gradient

SOLUTION OF THE PROBLEM

The expression for the velocity, u obtained as the solution of Eq. 2 subject to the boundary conditions 3 and Eq. 4 is obtained as (for $R_P \le r \le (z)$):

$$u = \frac{R_0^2}{4\mu}(-\frac{dp}{dz})((R/R_0)^2 - (r/R_0)^2) + (\tau_0 R_0/\mu)$$

$$((R/R_0) - (r/R_0)) - (4R_0^{3/2}\tau_0/3\mu) \tag{5}$$

$$(-\frac{1}{2\mu}\frac{dp}{dz})^{1/2}((R/R_0)^{3/2} - (r/R_0)^{3/2})$$

The constant plug flow velocity, u_P may be obtained from Eq. 5 evaluated at $r = R_P$. The volumetric flow rate Q can be defined as:

$$Q = \int_0^R 2\pi\, u\, r\, dr = \pi \int_0^R r\left(-\frac{du}{dr}\right) dr \qquad (6)$$

The flow flux, Q when $R_P << R$ (the radius of the plug flow region is very small as compared to the non-plug flow region) is calculated as:

$$Q = \frac{R_0^4 \pi}{8\mu}\left(-\frac{dp}{dz}\right)(R/R_0)^4 + -\frac{\tau_0 \pi}{3\mu}(R/R_0)^3 + $$
$$-\frac{4R_0^{7/2}\pi}{7}\left\{\frac{\tau_0}{\mu^2}\frac{1}{2}\left(-\frac{dp}{dz}\right)(R/R_0)^7\right\}^{1/2} \qquad (7)$$

$$Q = \frac{\pi R_0}{8\mu}\left(-\frac{dp}{dz}\right) f(\bar{y}) \qquad (8)$$

From above equation pressure gradient is written as follows:

$$\left(-\frac{dp}{dz}\right) = \frac{8\mu Q}{\pi R_0^4} f(\bar{y})$$
$$f(\bar{y}) = \left(\bar{y}\right)^4 + -\frac{\tau_0 \pi}{3\mu}\left(\bar{y}\right)^3 + \qquad (9)$$
$$-\frac{4R_0^{7/2}\pi}{7}\left\{\frac{\tau_0}{\mu}\left(-\frac{1}{2\mu}\frac{dp}{dz}\right)\left(\bar{y}\right)^7\right\}$$

Integrating Eq. 9 using the condition 3 $P = P_0$ at $z = 0$ and $P = P_L$ at $z = L$. We have:

$$\Delta P = P_L - P_0 = \frac{8\mu Q}{\pi R_0^4}\int_0^L \frac{dz}{(R(z)/R_0)^4 f(\bar{y}(z))} \qquad (10)$$

The resistance to flow is denoted by λ and defined as follows:

$$\lambda = \frac{P_L - P_0}{Q} \qquad (11)$$

The resistance to flow from Eq. 11 using Eq. 10 is written as:

$$\lambda = 1 - \left(L_0/L\right) + \left(f_0/L\right)\int_d^{d+L_0}\frac{dz}{(R(z)/R_0)^4 f(\bar{y}(z))} \qquad (12)$$

Where, f_0 is given by:

$$f_0 = \left(R/R_0\right)^4 + -\frac{\tau_0 \pi}{3\mu}\left(R/R_0\right)^3 + $$
$$-\frac{4R_0^{7/2}\pi}{7}\left\{\frac{\tau_0}{\mu}\left(-\frac{1}{2\mu}\frac{dp}{dz}\right)\left(R/R_0\right)^7\right\}$$

Following the apparent viscosity (μ_{app}) is defined as follows:

$$\mu_{app} = \frac{1}{\left(R(z)/R_0\right)^4 f(\bar{y})} \qquad (13)$$

The shearing stress at the wall can be defined as:

$$\tau_R = \tau_0 + \mu\left(-\frac{du}{dr}\right)_{r=R(z)} \qquad (14)$$

In order to have estimate of the quantitative effects of various parameters involved in the analysis computer codes were developed and to evaluate the analytical results obtained for resistance to blood flow, apparent viscosity and wall shear stress for normal and diseased system associated with stenosis due to the local deposition of lipids have been determine.

Figure 3 shows the variation of resistance to flow (λ) with stenosis size (δ/R_0) for different values of flow behavior index (n). It is observed that the resistance to flow (λ) increases as stenosis size (δ/R_0) increases. It is also noticed here that resistance to flow (λ) increases as flow behavior index (n) increases. It is seen from the Fig. 3 and 4 that the ratio is always >1 and decreases as n decreases from unity. This result is similar with the result of Shukla *et al.* (1980). In Fig. 4, resistance to flow (λ) decreases as stenosis shape parameter (m) increases and maximum resistance to flow (λ) occurs at (m = 2) in case of symmetric stenosis. This result is therefore consisting to the result of Haldar (1985). Figure 5 reveals the variation
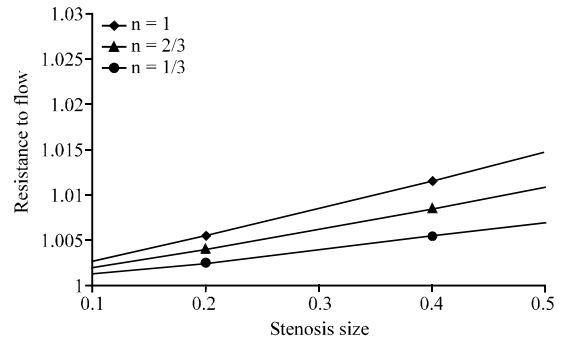

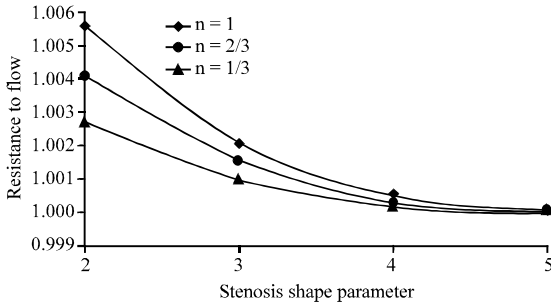Fig. 3: Variation of resistance to flow with stenosis size for different values of n

Fig. 4: Variation of resistance to flow with stenosis shape parameter for n
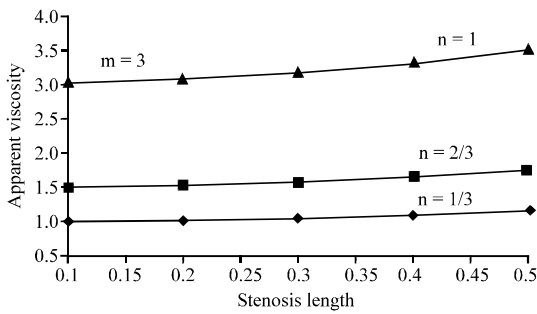

Fig. 5: Variation of apparent viscosity with stenosis lenght for different values of n

of apparent viscosity with stenosis shape parameter for different values of stenosis size. It may be observed here that the apparent viscosity decreases as stenosis shape parameter increases.

Figure 5 is also shows that apparent viscosity decreases as stenosis size increases. In Fig. 6 the variation of wall shear stress (τ) with stenosis length (L_0/L) for different values of flow behavior index (n) has been shown. Figure 6 shows that wall shear stress (τ) increases as stenosis length (L_0/L) increases. Also, it has been seen from this graph that the wall shear stress (τ) increases as value of flow behavior index (n) increases. As the stenosis grows, the wall shearing stress (τ) increases in the stenotic region. It is also noted that the shear ratio given by Lih (1975) is >1 and decreases as n decreases (n<1). These results are similar with the results of Shukla *et al.* (1980). It is also seen that the shear ratio is always >1 and decreases as n decreases. For $\delta/R_0 = 0.1$ the increases in wall shear due to stenosis is about 37% when compared to the wall shear corresponding to the normal artery in the Newtonian case (n = 1) but for n = 2/3 this increase is only 23% approximately. However, for $\delta/R_0 = 0.2$, the corresponding increase in Newtonian (n = 1) and non-Newtonian (n = 2/3) cases are 95 and 56%, respectively.
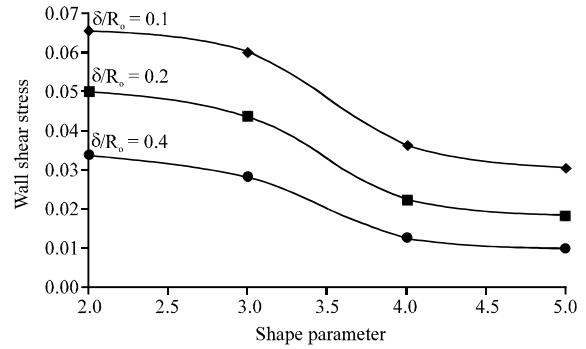

Fig. 6: Variation of wall shear stress with different values of stenosis size

CASSON'S FLUID MODEL

The Casson's relation is commonly written as:

$$\tau^{1/2} = \tau_0^{1/2} + (\mu)^{1/2}(-\frac{du}{dr})^{1/2}, \quad \text{if } \tau \geq \tau_0 \tag{15}$$

$$\left(\frac{du}{dr}\right) = 0 \quad \text{if } \tau < \tau_0 \tag{16}$$

Where:
R_c = The radius of the plug-flow region
τ_0 = Yield stress
τ = Wall shear stress
μ = Casson's viscosity coefficient

The volume rate of flow using Eq. 16 is defined as:

$$Q = \pi \int_0^R r^2 (-\frac{du}{dr}) dr \tag{17}$$

By integrating Eq. 17 using Eq. 16 and 3 we have:

$$Q = \frac{\pi R^4}{8\mu}\left(-\frac{dp}{dz}\right)\left[1 - \frac{16}{7}\left(\frac{R_c}{R}\right)^{1/2} + \frac{4}{3}\left(\frac{R_c}{R}\right) - \frac{1}{21}\left(\frac{R_c}{R}\right)^4\right], \tag{18}$$

Equation 18 can be rewritten as:

$$Q = \frac{\pi R^4}{8\mu}\left(-\frac{dp}{dz}\right)f(\overline{y})$$

Where:

$$f(\overline{y}) = \left[1 - \frac{16}{7}(\overline{y})^{1/2} + \frac{4}{3}(\overline{y}) - \frac{1}{21}(\overline{y})^4\right]$$

With:

$$\overline{y} = \frac{R_c}{R} \ll 1$$

From above equation pressure gradient is written as follows:

$$\left(-\frac{dp}{dz}\right) = \frac{8\mu Q}{\pi R^4 f(\overline{y})} \qquad (19)$$

Integrating Eq. 19 using the condition $P = P_0$ at $z = 0$ and $P = P_L$ at $z = L$. We have:

$$\Delta P = P_L - P_0 = \frac{8\mu Q}{pR_0^4} \int_0^L \frac{dz}{(R(z)/R_0)^4 f(\overline{y}(z))} \qquad (20)$$

The resistance to flow (resistive impedance) is denoted by λ and defined as follows (Young, 1968):

$$\lambda = \frac{P_L - P_0}{Q} \qquad (21)$$

The resistance to flow from Eq. 21 using Eq. 20 is written as:

$$\lambda = 1 - \frac{L_0}{L} + \frac{f_0}{L} \int_d^{d+L_0} \frac{dz}{(R(z)/R_0)^4 f(\overline{y}(z))} \qquad (22)$$

Where, f_0 is given by:

$$f_0 = \left[1 - \frac{16}{7}\left(\frac{R_c}{R_0}\right)^{1/2} + \frac{4}{3}\left(\frac{R_c}{R_0}\right) - \frac{1}{21}\left(\frac{R_c}{R_0}\right)^4\right]$$

Following the apparent viscosity (μ_{app}) is defined as follows:

$$\mu_{app} = \frac{1}{(R(z)/R_0)^4 f(\overline{y})} \qquad (23)$$

The shearing stress at the wall can be defined as:

$$\tau_R = \left[\tau_0^{1/2} + \left(-\mu\frac{du}{dr}\right)^{1/2}_{r=R(z)}\right]^2 \qquad (24)$$

Figure 7 shows the distributions of resistance to flow (λ) with stenosis size (δ/R_0) for different values of stenosis shape parameter (m). It is seen from the figure that the resistance to flow (λ) is always greater than unity and increases as stenosis size (δ/R_0) increases and decreases as the stenosis shape parameter (m) increases. Maximum resistance to flow (λ) occurs at m = 2 in the case of symmetric stenosis. This result is therefore, consistent
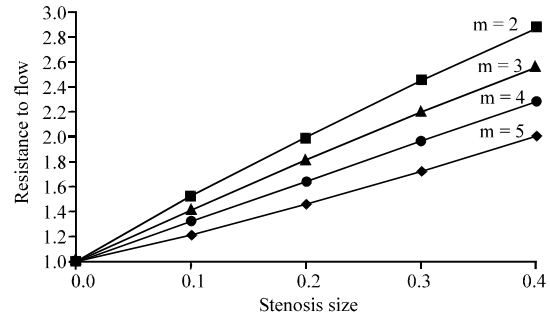

Fig. 7: Variation of resistance to flow with stenosis size for different value of stenosis shape parameter
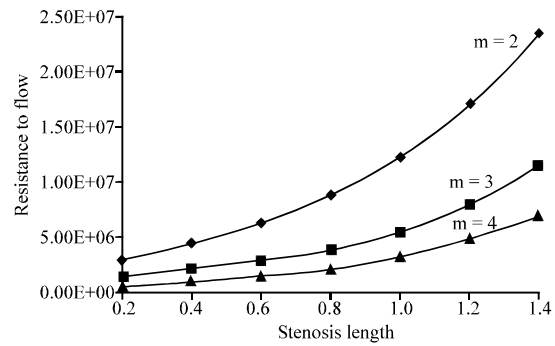

Fig. 8: Variation of resistance to flow with stenosis length for different values of stenosis shape parameter
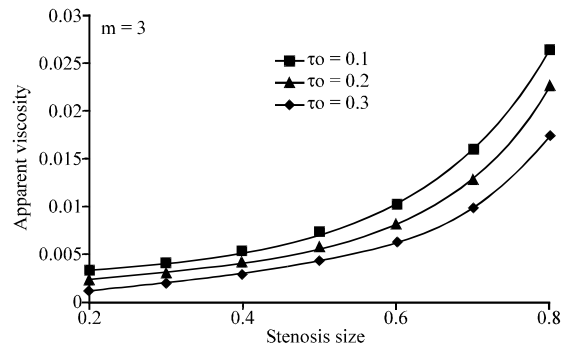

Fig. 9: Variation of apparent viscosity with stenosis size for different values of yield stress

with the observation of Haldar (1985). Figure 8 shows the variation of resistance to flow (λ) with stenosis length (L_0/L) for different values of stenosis shape parameter (m). Figure 8 shows that resistance to flow (λ) increases as stenosis length (L_0/L) increases and decreases as stenosis shape parameter (m) increases. This result is qualitative agreement with the observation of Haldar (1985).

Figure 9 shows variation of apparent viscosity (μ_{app}) with stenosis size (δ/R_0) for different values of yield stress
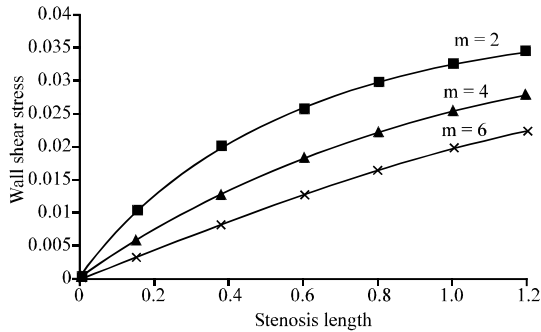
Fig. 10: Variation of wall shear stress with stenosis length for different values of stenosis shape parameter

(τ_0). Figure 9 shows that apparent viscosity (μ_{app}) increases as stenosis size (δ/R_0) increases but this increase is less due to non-Newtonian behaviour of the blodd. In addition it may be noted from the graph that the apparent viscosity (μ_{app}) decreases as yield stress (τ_0) increases. This result is in qualitative agreement with the result of Pontrelli (2001). It may be observed that from these results that the apparent viscosity increases as the stenosis grows and remains constants outside from the stenotic region. Figure 10 shows the variation of wall shear stress with stenosis length (L_0/L) for different values of stenosis shape parameter (m). Researchers observe that the wall shear stress sharply increases as length of stenosis (L_0/L) increases and decreases as stenosis shape parameter (m) increases. Tandon *et al.* (1991) have also noted the same results.

CONCLUSION

In this study, researchers have studied the effects of the stenosis in an artery by considering the blood as Bingham Plastic and Casson's Model fluids. It has been concluded that the resistance to flow and wall shear stress increases as the size of stenosis increases for a given Non-Newtonian Model of the blood. These increases are however, small due to non-Newtonian behaviour of the blood. It is noted that the non-Newtonian behaviour only slightly affects the pressure distribution. The results also indicate that as the degree of the stenosis area severity increases, the pressure gradient required to impel the blood passing through the narrowing channel increases significantly. This results in a higher pressure to occur in the up-stream region. The results clearly show how blood pressure increases as the degree of the stenosis severity increases. The non-Newtonian behaviour has very significant effect on the magnitude of wall shear stresses.

REFERENCES

Caro, C.G., J.M. Fitz-Gerald and R.C. Schroter, 1971. Atheroma and arterial wall shear observation, correlation and proposal of a shear dependent mass transfer mechanism for *Atherogenesis*. Proc. R. Soc., 177: 109-159.

Casson, N.A., 1959. Flow Equation for Pigment Oil Suspensions of the Printing Ink Type. In: Rheology of Disperse Systems, Mill, C.C. (Ed.). Pergamon Press, London, pp: 84-102.

Charm, S., 1965. Viscometry of human blood for shear rate of 100,000sec-1. Nature, 206: 617-618.

Cokelet, G.R., 1972. The Rheology of Human Blood. In: Biomechanics, Fung, Y.C.B., N. Perrone and M. Anliker (Eds.). Prentice-Hall, Englewood Cliffs, New Jersey, USA.

Forrester, J.H. and D.F. Young, 1970. Flow through a converging diverging tube and its implications in occlusive vascular disease. J. Biomech., 3: 297-316.

Fry, D.L., 1972. Localizing Factor In Arteriosclerosis, In atherosclerosis and Coronary Heart Disease. Grune Stratton, NewYork, Pages: 85.

Haldar, K., 1985. Effects of the shape of stenosis on the resistance to blood flow through an artery. Bull. Math. Biol., 47: 545-550.

Hershey, D. and S.J. Cho, 1966. Blood flow in ridig tubes: Thickness and slip velocity of plasma film at the wall. J. Appl. Physiol., 21: 27-32.

Jung, H., J.W. Choil and C.G. Park, 2004. Asymmetric flows of non-Newtonian fluids in symmetric stenosed artey. Korea Aust. Rheol. J., 16: 101-108.

Kirkeeide, R.L., D.F. Young and N.R. Chalvin, 1977. Wall vibrations induced by flow through simulated stenos arteries. J. Biomech., 10: 431-437.

LaBarbera, M., 1990. Principles of design of fluid transport systems in zoology. Science, 249: 992-1000.

Lee, J.S., 1974. On the coupling and detection of motion between an artery with a localized lesion and its surrounding tissue. J. Biomech., 7: 403-409.

Lih, M.M., 1975. Transport Phenomena in Medicine and Biology. John Wiley and Sons, New York.

May, A.G., J.A. Deweese and C.G. Rob, 1963. Hemodynamic effects of arterial stenosis. Surgery, 53: 513-524.

Pontrelli, G., 2001. Blood flow through an axisymmetric stenosis. Proc. Inst. Mech. Eng. H, 215: 1-10.

Reiner, M. and G.W.S. Baldair, 1959. The flow of the blood through narrow tubes. Nature, 184: 354-359.

Shukla, J.B., S.P. Gupta and R.S. Parihar, 1980. Biorheological aspects of blood flow through artery with mild stenosis: Effects of peripheral layer. Biorheology, 17: 403-410.

Tandon, P.N., P. Nirmala, M. Tewari and U.S. Rana, 1991. Analysis of nutritional transport through a capillary: Normal and stenosed. Comput. Math. Appl., 22: 3-13.

Texon, M., 1957. A homodynamic concept of atherosclerosis with particular reference to coronary occlusion. AMA Arch. Intern. Med., 99: 418-427.

Whitmore, R.L., 1968. Rheology of the Circulation. Pergamon Press, Oxford, Pages: 196.

Young, D.F. and F.Y. Tsai, 1973. Flow characteristics in models of arterial stenosis-II. unsteady flow. J. Biomech., 6: 547-559.

Young, D.F., 1968. Effects of a time-dependent stenosis on flow through a tube. J. Eng. Ind. Trans. AMSE., 90: 248-254.